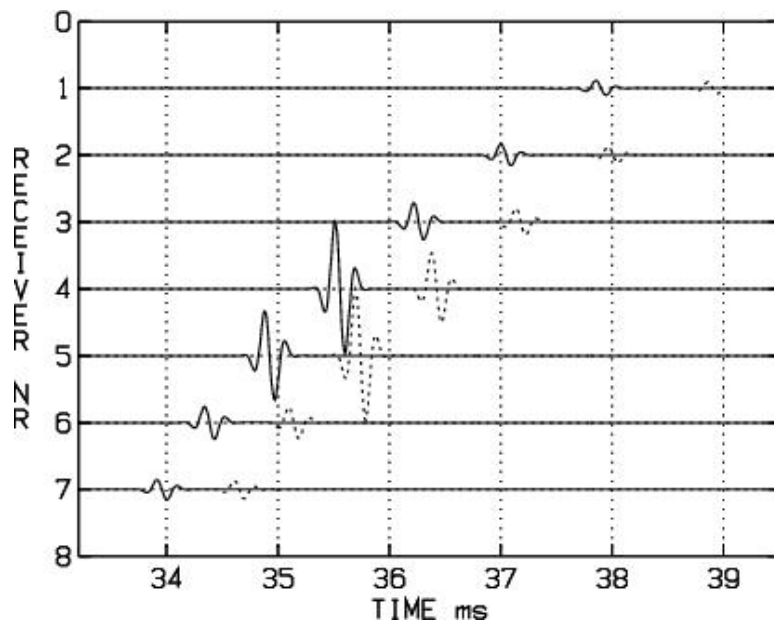


Mia Bondelind

Identification of object parameters from acoustic scattering data



SWEDISH DEFENCE RESEARCH AGENCY

Systems Technology
SE-164 90 Stockholm

FOI-R--1702--SE

October 2005

ISSN 1650-1942

Technical report

Mia Bondelind

Identification of object parameters from acoustic scattering data

Issuing organization FOI – Swedish Defence Research Agency Systems Technology SE-164 90 Stockholm	Report number, ISRN	Report type
	FOI-R--1702--SE	Technical report
	Research area code	
	4. C4ISTAR	
	Month year	Project no.
October 2005	E6058	
Sub area code		
43 Underwater Surveillance, Target acquisition and Reconnaissance		
Sub area code 2		
Author/s (editor/s) Mia Bondelind	Project manager	
	Henrik Claesson	
	Approved by	
	Monica Dahlén	
Sponsoring agency		
Swedish Armed Forces		
Scientifically and technically responsible		
Ilkka Karasalo		
Report title		
Identification of object parameters from acoustic scattering data		
Abstract (not more than 200 words) This paper describes computational analysis of the problem of estimating physical parameters of an object, buried in the seafloor, by acoustic probing. A ROV-mounted directive acoustic source sends a train of pulses at the object and the reflected echoes are registered by a separately located vertical receiver array. The fitness function then estimates the misfit between the experimentally observed and model-predicted time-series. Only model computations have been performed i.e. no experimental data have been used. Seven parameters describing the range, depth, roll, yaw, pitch, density and the sound speed of a box-shaped scatterer have been studied. The nonlinear global optimization problem has been solved with the Differential Evolution algorithm, DE. The local behaviour of the object function has been studied by evaluations of the second derivative at the global minimum. The Neighbourhood Algorithm Bayes, NAB, has been used to estimate the probability density function of the ensemble of parameter vectors.		
Keywords Acoustic scattering, bistatic, identification		
Further bibliographic information	Language English	
ISSN 1650-1942	Pages 21 p.	
	Price acc. to pricelist	

Utgivare FOI - Totalförsvarets forskningsinstitut Systemteknik 164 90 Stockholm	Rapportnummer, ISRN FOI-R--1702--SE	Klassificering Teknisk rapport
	Forskningsområde 4. Ledning, informationsteknik och sensorer	
	Månad, år Oktober 2005	Projektnummer E6058
	Delområde 43 Undervattenssensorer	
	Delområde 2	
Författare/redaktör Mia Bondelind	Projektledare Henrik Claesson	
	Godkänd av Monica Dahlén	
	Uppdragsgivare/kundbeteckning Försvarsmakten	
	Tekniskt och/eller vetenskapligt ansvarig Ilkka Karasalo	
Rapportens titel (i översättning) Identifiering av objektparametrar ur akustiska spridningsdata		
Sammanfattning (högst 200 ord) Studier av problemet att bestämma fysikaliska parametrar för ett begravt objekt på havsbotten genom inversion från akustiska spridningsdata beskrivs i rapporten. En ROV-buren akustisk källa sänder ett pulståg riktat mot ett objekt och de reflekterade ekona registreras av en separat placerad vertikal mottagarkedja. Fitness funktionen mäter sedan avvikelserna mellan de experimentellt observerade och numeriskt predikterade tidsserierna. Endast modell beräkningar har utförts dvs inga experimentella data har använts. Sju parametrar beskrivandes avstånd, djup, roll, yaw, pitch, täthet och ljudhastighet för objektet har studerats. Det globala icke-linjära optimeringsproblemet har lösts med en Differential Evolution, DE, algoritm. Lokalt beteende hos objektfunktionen har undersökts genom studier av andraderivatan vid det globala minimumet. The Neighbourhood Algorithm Bayes, NAB, har använts för att uppskatta sannolikhetsfördelningen för ensemblen av parametervektorer.		
Nyckelord Akustisk spridning, bistatisk, identifiering		
Övriga bibliografiska uppgifter	Språk Engelska	
ISSN 1650-1942	Antal sidor: 21 s.	
Distribution enligt missiv	Pris: Enligt prislista	

Acknowledgements

I would like to thank the following persons

- ★ My supervisor and examiner Ilkka Karasalo for his support and encouragement.
- ★ Sven Ivansson for his help with NAB.
- ★ Malcom Samebridge for making the NAB code available.
- ★ And finally my family for always believing in me.

Contents

1	Introduction	2
2	Parameter search regions	3
3	Object function	4
4	Differential Evolution	4
5	Tools for evaluation of results	6
5.1	Local behaviour of the object function $\Phi(\mathbf{u})$	6
5.2	Neighbourhood Algorithm Bayes	6
6	Results	8
6.1	Structuring the parameter space	8
6.2	Differential Evolution	11
6.3	Local behaviour of the object function $\Phi(\mathbf{u})$	13
6.4	Neighbourhood Algorithm Bayes	15
7	A final test	17
8	Discussion	19
9	Conclusions	20

1 Introduction

This paper describes computational analysis of the problem of estimating physical parameters of an object buried in the seafloor by acoustic probing. For a more thorough description of the background see [5].

A ROV-mounted directive acoustic source sends a train of pulses at the object and the reflected echoes are registered by a separately located vertical receiver array as shown in figure 1.

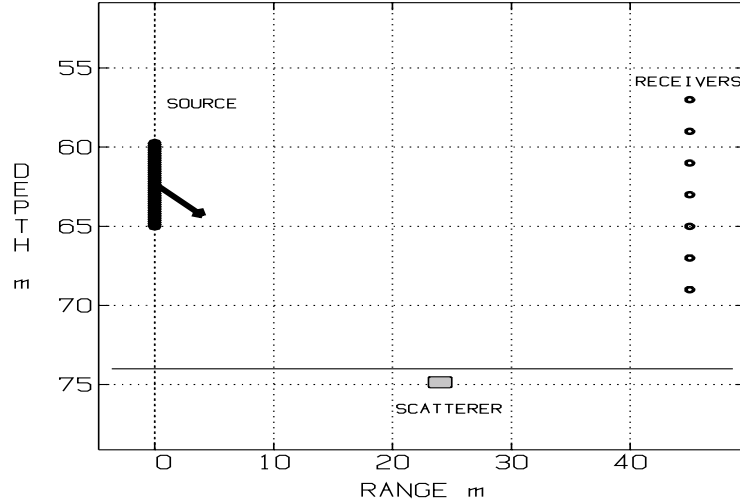


Figure 1: *Experimental geometry.*

The scatterer has the shape of a homogeneous super-ellipsoid with acoustic parameters representative of a TNT explosive, density 1630 kg/m^3 and sound speed 2680 m/s , figure 2.

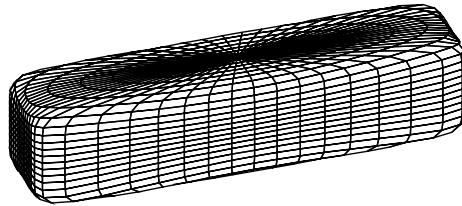


Figure 2: *Shape of the scatterer, a super-ellipsoid with half-axes 65, 15 and 15 cm.*

Seven parameters, describing the range, depth, roll, yaw, pitch, density and sound speed of the scatterer, have been studied. A coordinate system is defined with upward pointing z axis passing through the source point and the positive x axis directed towards the scatterer and the receivers. The angles, roll, pitch and yaw will then be defined as the rotations around the x , y and z axes of the coordinate system.

The signals at the receivers for a given parameter combination are computed by a fast hybrid method based on ray tracing and plane wave reflection and transmission coefficients. An example can be seen in figure 3 showing the signals

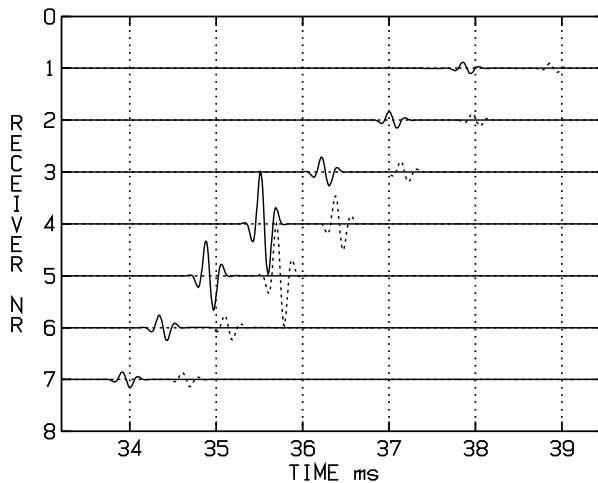


Figure 3: *Model-predicted signals corresponding to two different points in the search domain. Range = 24.0 m and Depth = 74.85 m i.e. the true values (Solid line). Range = 24.3 m and Depth = 76.0 m (Dashed line). The other parameters have been kept constant at true values, table 1.*

at each receiver for two different locations of the centre of the scatterer. The program has been executed on a 23-node linux cluster.

The optimization problem arises when a set of parameters are to be determined from experimental measurements of a scattered field registered at the receivers. The parameters are estimated by minimizing a measure of the misfit between the experimentally observed and the model-predicted signals. The sought parameter combination arises from the model-predicted signal that results in the lowest misfit value. In this paper only model computations have been performed i.e. no experimental data have been used. Noise is therefore not present in the calculations which makes the results very precise.

To solve the nonlinear global optimization problem effectively an evolutionary algorithm the so called Differential Evolution, DE, has been implemented and used. Differential evolution was introduced a few years ago by Price and Storn [7], and has shown to be successful in solving problems with a highly nonlinear object function consisting of many local minima. The results have thereafter been evaluated by studies of the second derivative of the object function at the global minimum and by resampling of the ensemble with the Neighbourhood Algorithm Bayes, NAB, [8].

2 Parameter search regions

Actual experimental data for the arrival time τ and the amplitude α at the receivers have not been used during the optimization and model input data had to be created. The parameter values stated in the “Original” column of table 1 were chosen, the corresponding transient echoes were calculated and used as simulated experimental data in the fitness function. As a result not only τ and α are known but also the correct parameter values corresponding to the signal. These parameter values are called *original* or *true* values.

	Min	Max	Original
Range (<i>m</i>)	18	31	24
Depth (<i>m</i>)	74.16	76	74.85
Roll (<i>deg</i>)	-5	5	0
Yaw (<i>deg</i>)	15	25	19
Pitch (<i>deg</i>)	-5	5	0
Density (<i>kg/m³</i>)	1400	1800	1630
Sound speed (<i>m/s</i>)	2300	2700	2680

Table 1: Search domain and the original parameter values.

Table 1 shows the search region and the original parameter values used throughout this study.

3 Object function

The fitness function, eq (1), is a measure of the misfit between the experimentally observed time-series, in this case the modelled experimental input data, and the model-predicted time-series.

$$\Phi(\mathbf{u}) = \sum_{i=1}^N \left| \frac{T_i(\mathbf{u}) - \tau_i}{T_{scal}} \right|^2 + \left| \frac{A_i(\mathbf{u}) - \alpha_i}{A_{scal}} \right|^2 \quad (1)$$

The arrival times τ_i and the amplitudes α_i at the receivers are those of the simulated experimental data. $T_i(\mathbf{u})$ and $A_i(\mathbf{u})$ are the modelled arrival time and the amplitude, respectively, at receiver i as function of the parameter vector \mathbf{u} .

It is desirable for the two terms in the function to be of the same order of magnitude so that neither of the terms dominates the fitness value. The function turned out to be very sensitive to scaling and this was therefore more thoroughly examined. Among several different scalings two of the best were

Scaling :	Time	Amplitude
S_1	$T_{scal} = 1$	$A_{scal} = \max_i \alpha_i$
S_2	$T_{scal} = \max_i \tau_i - \min_i \tau_i$	$A_{scal} = \max_i \alpha_i$

The two different scalings, S_1 and S_2 , gave almost the same results. Both kept the difference in magnitude of the two terms in the object function at an acceptable level. The S_2 scaling has been used throughout this thesis.

4 Differential Evolution

The fitness function is in general a complicated nonlinear function, possibly with several local minima. The optimal parameter combination must be sought by methods for nonlinear global optimization. Differential Evolution, from here on

referred to as DE, is a relatively new evolutionary algorithm proposed by Storn and Price [7].

The method described below is one of many variants of the DE algorithm, though the difference between them is small. The algorithm is easy to work with since only a few control variables exist and they remain fixed through the entire optimization procedure [10]. Another advantage with the DE algorithm is that the size of the population remains constant during the optimization process. The initial population, P_1 , consists of randomly chosen parameter vectors u_i^1 , where

$$u_i^1 = (u_{i,1}^1, \dots, u_{i,D}^1), \quad i = 1, \dots, N.$$

After g generations the population can then be written as

$$P_g = \{u_1^g, \dots, u_N^g\}.$$

The next population P_{g+1} is calculated in two steps. First a set of trial vectors

$$P_{g+1,tri} = \{v_1^{g+1}, \dots, v_N^{g+1}\}.$$

is computed, where the i 'th trial vector v_i^{g+1} is obtained by choosing a random component number $k_i \in \{1, \dots, D\}$, and by selecting random numbers p, q, r , not equal to each other nor equal to i . Then for each element in $v_{j,i}^{g+1}$

$$v_{j,i}^{g+1} = \begin{cases} u_{j,p}^g + F \cdot (u_{j,q}^g - u_{j,r}^g) + n_j \cdot (b_j - a_j) & \text{if } R_j \leq CR \text{ or } j = k_i \\ u_{j,i}^g & \text{otherwise} \end{cases}$$

where $j = \{1, \dots, D\}$ and F and CR are constant parameters with values in $(0, 1]$ though usually they are in the range of $[0.5, 1]$. R_j is a uniformly distributed random number. $[a_j, b_j]$ is the search interval of parameter vector component j and n_j is an integer such that $v_{j,i}^{g+1}$ stays inside the search region, $v_{j,i}^{g+1} \in [a_j, b_j]$. A uniform probability distribution has been assumed for all random decisions. There are many different schemes to acquire the i 'th trial vector, this choice is based on studies of the DE algorithm done by Rune Westin [3].

The new population is obtained by comparing the individuals from the current and the trial populations according to

$$u_i^{g+1} = \begin{cases} v_i^{g+1} & \text{if } \Phi(v_i^{g+1}) < \Phi(u_i^g) \\ u_i^g & \text{otherwise} \end{cases} \quad (2)$$

New populations are generated until DE is terminated by fulfilling a stopping criteria chosen a priori, eg. the decrease of the fitness value is less than a given tolerance or the number of new individuals generated in the latest 10 generations is zero.

The control variables, F and CR , influence the convergence rate and the robustness of the algorithm. The optimal choice of F and CR depends on both the object function and the population size N [6]. In practice F and CR are tuned in by a few trial optimizations [11].

An advantage with DE is that the decision of accepting or rejecting a trial vector is based on comparing it with only one individual instead of all individuals in

the current population [6]. This makes DE more robust and tends to prevent it from getting caught in local minima.

5 Tools for evaluation of results

5.1 Local behaviour of the object function $\Phi(\mathbf{u})$

In a neighbourhood of its global minimum the fitness function $\Phi(\mathbf{u})$ can be written as

$$\Phi = \frac{1}{2}h^T H h + \Phi_{min} + O(h^3)$$

where H is the symmetric Hessian matrix [4]. If λ_i and v_i , $i = 1, \dots, D$ denote the eigenvalues and the orthogonal and normalized eigenvectors of H , then

$$H = V^T \Lambda V$$

where V is the orthogonal matrix

$$V = [v_1, \dots, v_D]$$

and Λ is the diagonal matrix

$$\Lambda = \text{diag}(\lambda_1, \dots, \lambda_D)$$

The fitness function can now be written as

$$\Phi = \frac{1}{2} \sum_j k_j^2 \lambda_j + \Phi_{min} + O(h^3)$$

where $k_j = V_j^T h$ [1]. Thus the eigenvalues and eigenvectors decompose the parameter space into parameter combinations where large eigenvalues indicate parameter combinations with large influence on the object function in a neighbourhood of the minimum point.

To study the sensitivity of the object function Φ , as function of the components of the parameter vector \mathbf{u} , the second partial derivatives of the fitness function were calculated by second-order central differences at the global minimum. The eigenvalues and the eigenvectors of the Hessian matrix were then computed by standard methods.

5.2 Neighbourhood Algorithm Bayes

After a completed parameter search the resulting set of models and their fitness values, can be used to gain information about the unknown probability distribution of the parameters. The Neighbourhood Algorithm Bayes, NAB, has been used to estimate the posterior probability density, PPD, of the samples generated by the DE algorithm. The resulting PPD depends upon the vectors chosen

by the DE algorithm, the fitness values and the statistics of all noise present. A short summary of the algorithm is given below. For a more thorough description see [3] and Sambridge [12] and [8].

In NAB all vectors, generated by the search method, are used since models that fit the data poorly are informative as well. An attractive feature of NAB is that no further solving of the forward problem has to be done. The algorithm needs only to know an a priori probability density for the ensemble of parameter vectors and an estimate of the distribution of the noise present in the data. The a priori probability density $\rho(\mathbf{u})$, at the point \mathbf{u} in model space, is chosen to be uniform within the search domain if no prior preferences of different locations in the search space exists. NAB then estimates the posterior probability density function, PPD, by resampling the parameter space. The PPD is thereafter displayed in the form of marginal distributions of the components of \mathbf{u} .

NAB requires the PPD of the noise to be known and in this study the noise has been assumed to be Gaussian with standard deviation σ . At any point \mathbf{u} in the model space the PPD is then proportional to

$$P(\mathbf{u}) \sim \rho(\mathbf{u}) \cdot e^{-\frac{\Phi(\mathbf{u})}{2\sigma^2}}$$

where $\Phi(\mathbf{u})$ is the fitness value obtained from eq (1) [3].

Voronoi cells

The PPD estimate computed by NAB is based on Voronoi cells. A Voronoi cell consists of all points \mathbf{u} in the parameter space that are closer to sample point \mathbf{u}_j than to any other sample point \mathbf{u}_k , $k \neq j$. A neighbourhood approximation of the PPD is derived by setting the known PPD of each model to be constant inside each Voronoi cell. In the resampled ensemble the density of points will be proportional to the PPD. In effect, each Voronoi cell acts as a 'neighbourhood of influence' about the corresponding point in the ensemble. Voronoi cells are unique, space filling and can adapt their size and shape to the distribution of the ensemble. This feature makes them very useful when working in any number of dimensions with any distribution of irregular points.

Gibbs sampling

The Gibbs sampler [2] [9] is used to generate the resampled ensemble. The method generates a random walk in model space, whose distribution asymptotically converges. In NAB Gibbs sampling is used to generate samples distributed according to the neighbourhood approximation of the PPD. The random walk is performed in a series of steps parallel to each parameter axis in turn. The walk can move into any intersecting Voronoi cell with probability determined by the product of the width of the intersection and the PPD value.

Convergence of the Gibbs sampler is required and can be monitored using standard statistical techniques. The reason for NABs efficiency is that no further solving of the forward problem has to be performed and that only the intersection with Voronoi cells along axis-parallel lines has to be calculated during the Gibbs sampling.

6 Results

6.1 Structuring the parameter space

The task has been to study the behaviour of the fitness function when being optimized and how different parameter combinations influence the object function. To handle the optimization problem the seven parameters were divided into three groups.

- A Range and Depth
- B Roll, Yaw and Pitch
- C Density and Sound speed

These groups were tested separately with DE as well as combinations of them, e.g. AB, BC and so forth. The behaviour of the object function Φ is markedly different depending on the parameter group used. Some of the more notable features are shown below.

Range and Depth

Range and Depth give rise to fitness values in the range of $[0, 87.4]$ and the minimum at Range 24.0 m, Depth 74.85 m is well defined. The minimum in the direction of the Depth parameter is stretched out a little, figure 4 and 5.

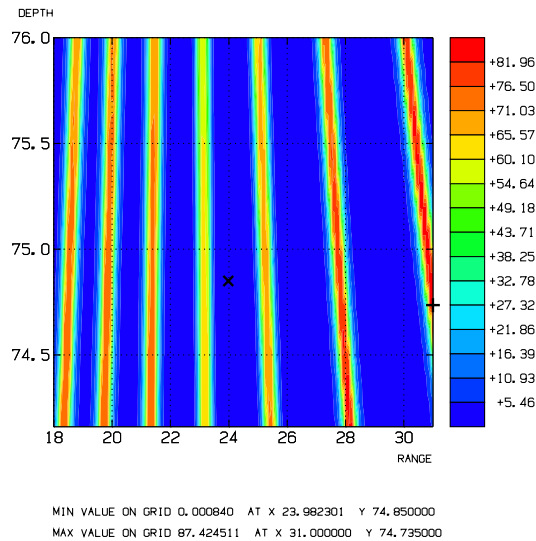


Figure 4: *The object function Φ as function of Range and Depth.*

Roll, Yaw and Pitch

The two angles, Roll and Pitch, have a large influence on the fitness function and show a well defined minimum. Only large yaw angles will influence the object function due to the box shaped scatterer and the source-receiver geometry see figure 1. Small changes in the yaw angle will have little effect on the fitness function, fig 6.

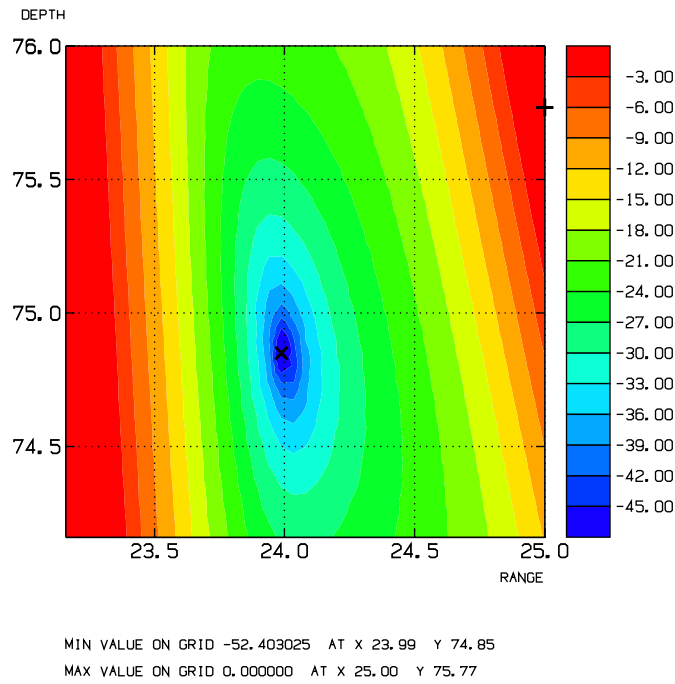


Figure 5: *The object function as function of Range and Depth. The figure is plotted with a decibel scale and a smaller boundary region has been used to show the area around the minimum (24.0, 74.85).*

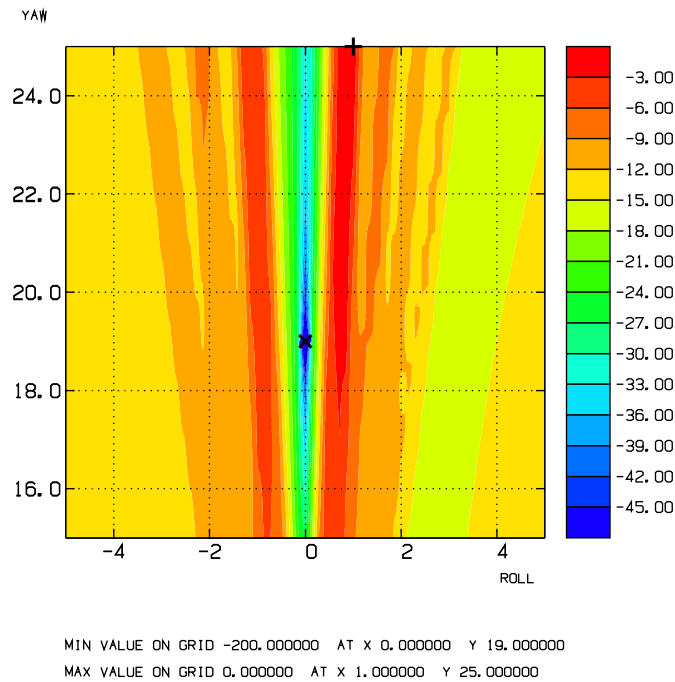


Figure 6: *The object function as function of Roll and Yaw. The figure is plotted with a decibel scale.*

Density and Sound speed

As seen in figure 7 changes of the Density and the Sound speed give rise to very small variations in the object function. The fitness values shows a shallow valley oriented along the SW-NE diagonal of the region, not along contours of the constant acoustic impedance ρc . A separate investigation not included in this report showed that for Density and Sound speed closer to the values of the water the contours of the object function will have the expected form $\rho c = \text{constant}$.

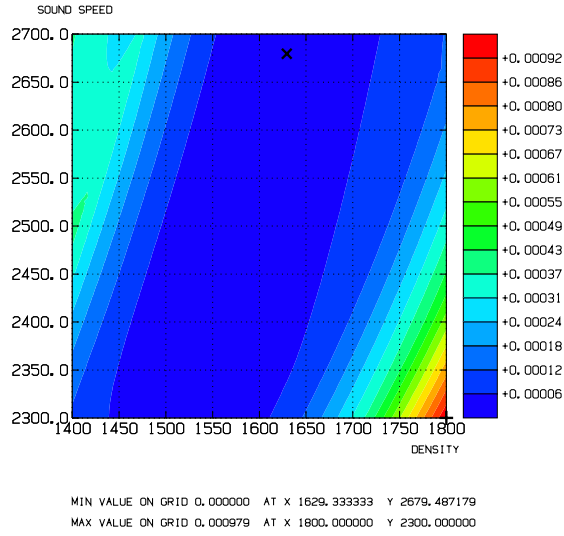


Figure 7: The object function as function of Density and Sound speed.

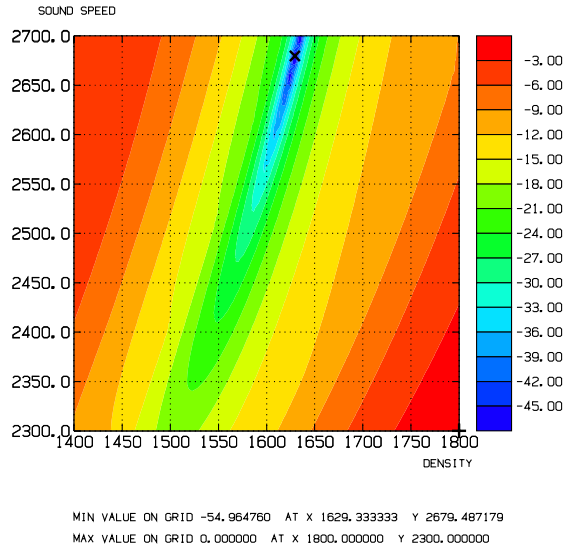


Figure 8: The object function as function of Density and Sound speed. A decibel scale has been used to better be able to show the shape of the figure.

6.2 Differential Evolution

Several trial optimizations were carried out to select optimal values for F , CR and N for the optimization problem studied here. The values obtained were $F = 0.5$ and $CR = 0.9$ with $N = 20$.

To terminate the DE algorithm two stopping criteria have been used

- the current population has not changed in 10 iterations.
- the fitness value is smaller than a given tolerance, tol .

Range and Depth

In the first group, A, the parameters were easily determined at a tolerance of $tol = 10^{-4}$, table 2. It might be noted that the Depth was slightly less correct than the Range parameter. This behaviour is to be expected in view of the elongated minimum in the Depth parameter direction seen in figure 5.

	Original	case A
Range	24.0	24.998
Depth	74.85	74.856

Table 2: *Optimized values for the parameters Range and Depth with the object function $\Phi(Range, Depth)$ with $tol = 10^{-4}$.*

Roll, Yaw and Pitch

Roll, Yaw and Pitch, case B, were also easy to determine with DE. Overall Roll and Pitch are better determined than the Yaw angle, table 3. This is because of the behaviour mentioned in section 6.1 and seen in figure 6.

	Original	case B	case B
tol	-	10^{-4}	10^{-6}
Roll	0	$6.54 \cdot 10^{-2}$	$3.50 \cdot 10^{-3}$
Yaw	19	18.98	19.01
Pitch	0	$-6.76 \cdot 10^{-2}$	$-3.47 \cdot 10^{-3}$

Table 3: *Optimized values for the parameters Roll, Yaw and Pitch with the fitness function $\Phi(Roll, Yaw, Pitch)$. Two separate runs are shown in the table where the tolerance has been varied.*

Range, Depth, Roll, Yaw and Pitch

When optimizing groups A and B jointly (i.e. the five parameters Range, Depth, Roll, Yaw and Pitch) convergence was slow and the minimum was difficult to reach. Increasing the tolerance does not improve the results since DE fulfils the first stopping criterion and therefore terminates without creating new individuals.

Density and Sound speed

Neither the Density nor the Sound speed influences the object function by much in the chosen domain giving rise to function values in the range of $[0, 10^{-3}]$, figure 7. They are therefore difficult to determine by DE minimization. Both parameters are well determined only if $tol \leq 10^{-9}$, however such small tolerances are not very meaningful since they would be far below the noise level in actual experimental data.

Comparing case AC with case BC

At a tolerance of 10^{-9} all four parameters in case AC can be determined. The smaller the tolerance the more difficult it is to reach convergence. When reaching a tolerance of 10^{-9} DE will still converge for the BC-case but it is not possible to determine the Density and the Sound speed as well as in the AC-case, see table 4.

	Original	case AC	case BC
Density	1630	1630.32	1634.69
Sound speed	2680	2680.35	2695.31
Tol	-	10^{-9}	10^{-9}

Table 4: *Parameter values for the Density and the Sound speed when optimizing case AC: with parameter Range, Depth, Density and Sound speed and case BC: with Roll, Yaw, Pitch, Density and Sound speed.*

All seven parameters

Larger tolerances had to be used to reach convergence when trying to optimize all parameters at once. The Density and the Sound speed did not converge to the original values and smaller search regions for the two parameters were tried however this did not improve the results.

	Original	DE results
Optimization 1:	43 iterations	
Range	24.0	24.0
Depth	74.85	74.85
Optimization 2:	81 iterations	
Roll	0	$-1.2 \cdot 10^{-4}$
Yaw	19.0	18.999
Pitch	0	$8.96 \cdot 10^{-5}$
Optimization 3:	19 iterations	
Density	1630.0	1629.7
Sound speed	2680.0	2679.3

Table 5: *Optimization by three parameter searches in sequence.*

If the optimization is carried out over the groups A, B and C in sequence, all searches converged to the true values, table 5. The results from the first

optimization is used in the second and then in the third, the Range, Depth, Roll, Yaw and the Pitch are kept constant with the obtained values from the previous runs. The tolerance, $tol = 10^{-9}$, was used in all three optimizations.

6.3 Local behaviour of the object function $\Phi(\mathbf{u})$

Range and Depth

The diagonal, the eigenvalues and the eigenvectors of the Hessian matrix at the global minimum are shown in table 6. It shows that Range have the most significant influence on the object function, and is therefore expected to converge more rapidly to the true value than Depth. The Depth parameter influences the fitness function less than Range and will converge slower and be slightly less accurate. This can also be seen in figure 4. However both parameters will be well determined and $\Phi(\text{Range}, \text{Depth})$ has a distinct minimum.

	Diagonal of H	Eigenvalues	Eigenvectors
$\frac{\partial^2 \Phi}{\partial \text{Range}^2}$	5.27	5.51	Range 1.00 -0.224
$\frac{\partial^2 \Phi}{\partial \text{Depth}^2}$	0.723	0.481	Depth 0.224 1.00

Table 6: The diagonal of the Hessian matrix, H , with corresponding eigenvalues and eigenvectors for $\Phi(\text{Range}, \text{Depth})$.

Roll, Yaw and Pitch

The second derivatives at the global minimum confirm that the fitness function is much less sensitive to Yaw than to the other two angles. Thus the Roll and Pitch angles are determined faster and more accurately by inversion than the Yaw angle table 7.

	Diagonal of H	Eigenvalues
$\frac{\partial^2 \Phi}{\partial \text{Roll}^2}$	2.77	6.05
$\frac{\partial^2 \Phi}{\partial Y_{gw}^2}$	1.3810^{-3}	1.2410^{-2}
$\frac{\partial^2 \Phi}{\partial \text{Pitch}^2}$	3.30	9.3810^{-5}

	Eigenvectors		
Roll	0.916	1.00	-0.210
Yaw	$9.94 \cdot 10^{-3}$	0.394	1.00
Pitch	1.00	-0.912	0.202

Table 7: The diagonal of the Hessian matrix, H , and corresponding eigenvalues and eigenvectors for the three angles Roll, Yaw and Pitch.

Range, Depth, Roll, Yaw and Pitch

Also optimizing with the five parameters Range, Depth and the three angles the Hessian matrix shows that Depth and Yaw are the two variables that will be most difficult to determine, table 9.

Density and Sound speed

The influence of the variables Density and Sound speed on the object function is very small and the function it self shows a faint slope at the global minimum, figure 7. The diagonal, the eigenvalues and the eigenvectors of H are shown in table 8. One eigenvalue of H is negative which can not hold at local minima in the absence of computational errors. This indicates that the variation of the fitness function with Density and Sound speed is smaller than the numerical errors arising at computations of Φ .

One should consider that these results holds for the search region and original values, shown in table 1. Both Density and Sound speed have a greater impact on the object function in a search region closer to the values of water, in this case 1000 respective 1438.

	Diagonal of H				Eigenvalues
$\frac{\partial^2 \Phi}{\partial Range^2}$	4.83				4.87
$\frac{\partial^2 \Phi}{\partial Depth^2}$	0.533				0.488
$\frac{\partial^2 \Phi}{\partial Density^2}$	2.1410^{-8}				1.5210^{-10}
$\frac{\partial^2 \Phi}{\partial Soundspeed^2}$	1.4710^{-9}				-2.8510^{-8}

	Eigenvectors			
Range	1.00	-0.102	$4.48 \cdot 10^{-6}$	$1.12 \cdot 10^{-4}$
Depth	0.102	1.00	$-1.45 \cdot 10^{-6}$	$-3.49 \cdot 10^{-5}$
Density	$-9.74 \cdot 10^{-5}$	$4.17 \cdot 10^{-5}$	0.357	1.00
Sound speed	$3.04 \cdot 10^{-5}$	$-1.30 \cdot 10^{-5}$	1.00	-0.357

Table 8: *The diagonal of the Hessian matrix, H , with corresponding eigenvalues and eigenvectors for the parameters Range, Depth, Density and Sound speed.*

All seven parameters

At a discretization step of $h = 0.001$ the derivative resembles the one obtained with the AB case since the Hessian matrix elements are zero in the rows and columns for Density and Sound speed, table 9. One way to find out how many of the parameters that can be expected to be determined by inversion is to plot the eigenvalues of the Hessian matrix and draw a line at the level of the noise. This is shown in figure 9 where three of the eigenvalues are seen to be well above the noise level. Thus three parameters are well determined by the data. The fourth eigenvalue is close to the noise level, dotted line, and the rest of the parameters will drown in noise.

	Diagonal of H	Eigenvalues
$\frac{\partial^2 \Phi}{\partial Range^2}$	5.27	11.5
$\frac{\partial^2 \Phi}{\partial Depth^2}$	7.23	0.505
$\frac{\partial^2 \Phi}{\partial Roll^2}$	2.77	3.1410^{-2}
$\frac{\partial^2 \Phi}{\partial Yaw^2}$	1.3810^{-3}	2.5210^{-3}
$\frac{\partial^2 \Phi}{\partial Pitch^2}$	3.30	0
$\frac{\partial^2 \Phi}{\partial Density^2}$	0.00	0
$\frac{\partial^2 \Phi}{\partial Soundspeed^2}$	0.00	-3.5810^{-5}

	Eigenvectors						
Range	1.00	-0.048	0.766	0.544	0.00	0.00	0.105
Depth	0.209	1.00	-0.0866	-0.0255	0.00	0.00	$1.16 \cdot 10^{-3}$
Roll	-0.722	0.120	1.00	-0.356	0.00	0.00	-0.273
Yaw	$8.23 \cdot 10^{-3}$	$-3.20 \cdot 10^{-4}$	0.179	-0.547	0.00	0.00	1.00
Pitch	-0.791	0.0942	0.0345	1.00	0.00	0.00	0.393
Density	-0.00	0.00	0.00	0.00	1.00	0.00	0.00
Sound speed	-0.00	0.00	0.00	0.00	0.00	1.00	0.00

Table 9: The diagonal of the Hessian matrix and the corresponding eigenvalues and eigenvectors of the Hessian matrix for all seven parameters.

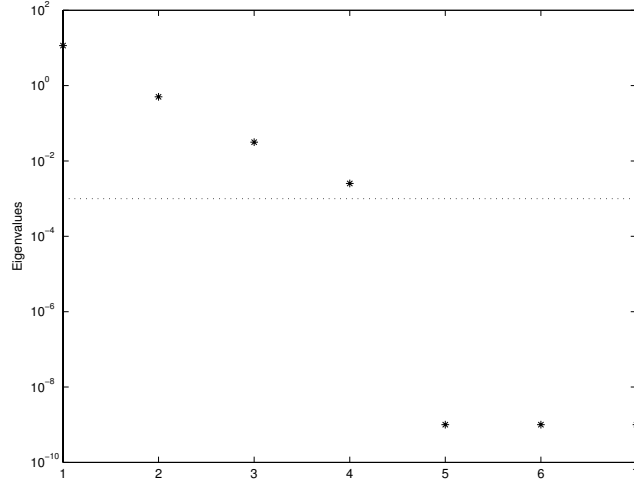


Figure 9: Eigenvalues from table 9. The dotted horizontal line represents the noise level.

6.4 Neighbourhood Algorithm Bayes

Two choices of ensembles, consisting of parameter vectors with corresponding fitness values, used as input to NAB were investigated: All trial vectors and only the accepted trial vectors, respectively, generated by the DE search. One difference between these ensembles is how densely they fill out the search region, see figure 11 and 10.

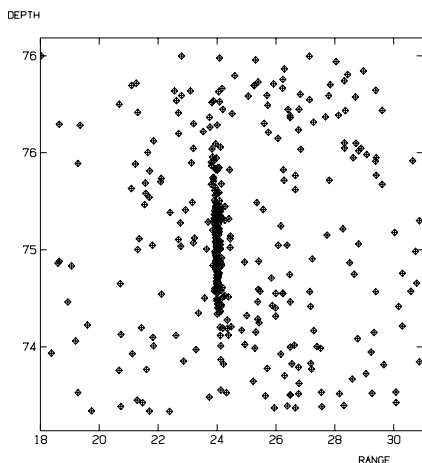


Figure 10: *The set of all trial vectors in a DE search.*

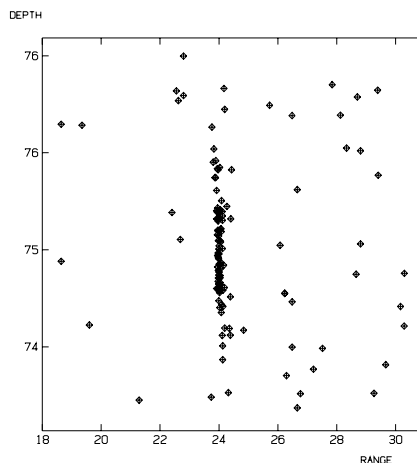


Figure 11: *The set of accepted trial vectors in a DE search, see eq (2).*

NAB is dependent on having sample points from the entire domain to produce accurate results. The algorithm also requires that the minimum (the area around the lowest misfit) has been well searched during the optimization. Therefore NAB has been run with a vector containing values from all generated trial vectors.

NAB assumes that noise is present in the data and this has therefore been added during the DE optimization. The added noise prevents DE from reaching as low tolerances as stated in section 6.2.

Range and Depth

Depth turns out not to be as well defined as the rest of the parameters when being resampled with the parameters Range, Roll, Yaw and Pitch, which can be seen in figure 12 and 13. This indicates that Depth will be harder to determine well than the other parameters. Range, on the other hand, is easily determined partly because of its sharp slope of the function, at the minimum, in the Range direction.

Roll, Yaw and Pitch

The angles cause no problem during the resampling and the resulting ensemble shows that Roll, Yaw and Pitch have been well determined during the DE optimization. The problem of reaching convergence with a low tolerance when running the DE algorithm, with noise added, seems not to have any influence of the accuracy of the angle parameters.

Range, Depth, Roll, Yaw and Pitch

The results from the DE optimization with $\Phi(\text{Range}, \text{Depth}, \text{Roll}, \text{Yaw}, \text{Pitch})$ showed that Yaw was not as well determined as the two other angles. This observation is confirmed by NAB, fig 12 and 13.

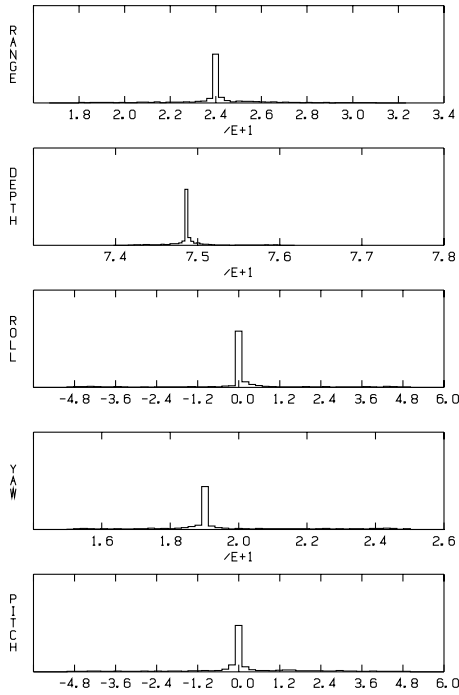


Figure 12: *1D marginal distribution by DE.*

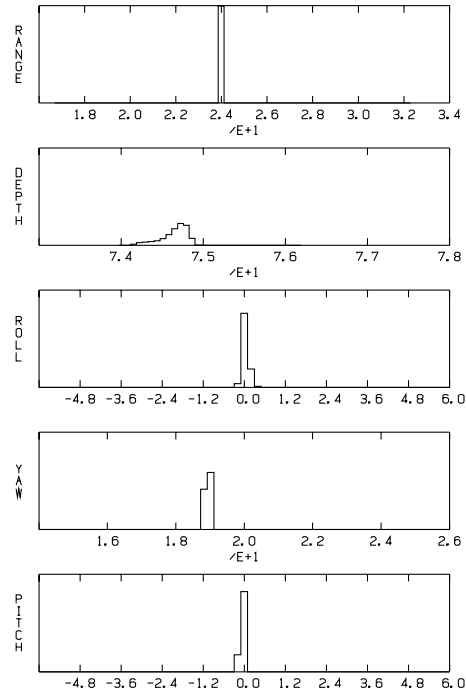


Figure 13: *1D marginal distribution by NAB.*

Density and Sound speed

The fitness values obtained from $\Phi(\text{Density}, \text{Sound speed})$ are very small and the parameters Density and Sound speed are therefore not determinable by inversion even without noise present. When noise was added the parameters became very hard to determine properly and the needed tolerance of 10^{-9} could not be reached.

The results presented by NAB are somewhat confusing when one or both of the Density and the Sound speed is present during the resampling. All other parameters involved will be claimed as indeterminable. This could be the case, but it is more likely that it is the Density and the Sound speed that are causing this since they are not well determined during the DE optimization.

7 A final test

The results obtained in the previous chapters indicate that perhaps $\Phi(\text{Range}, \text{Roll}, \text{Pitch})$ would give well defined results by a DE optimization. This was therefore tried and the following values was obtained, tab 10.

Due to the well defined global minimum of the fitness function and the high tolerance the DE does not have to search for long to find the optimal value of Φ . This results in fewer iterations with DE and thus fewer values in the resulting ensemble. The marginal distribution from the DE ensemble shows therefore only small peaks at the original values.

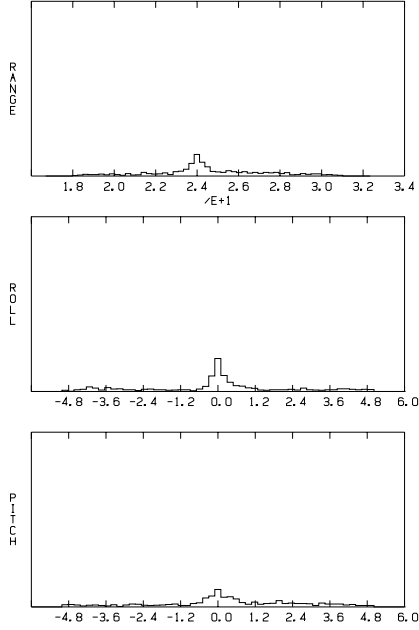


Figure 14: *1D marginal distribution by DE; from the top Range, Roll and Pitch.*

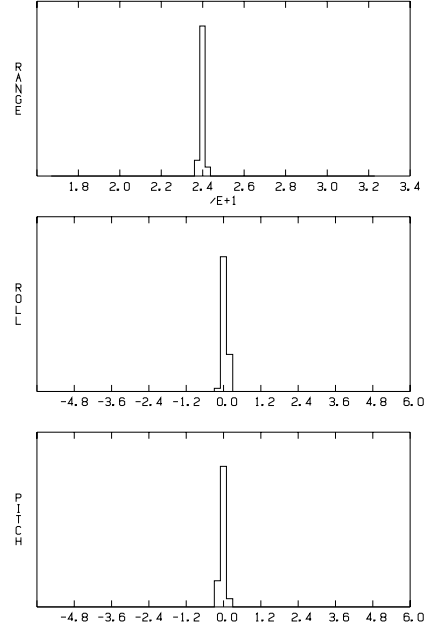


Figure 15: *1D marginal distribution by NAB; from the top Range, Roll and Pitch.*

	Original	DE values
Range	24.0	24.0
Roll	0	$9.89 \cdot 10^{-3}$
Pitch	0	$-7.06 \cdot 10^{-3}$
tol	-	10^{-5}

Table 10: *Optimized values for the parameters Range, Roll and Pitch with the fitness function $\Phi(\text{Range}, \text{Roll}, \text{Pitch})$.*

	Diagonal of H	Eigenvalues
$\frac{\partial^2 \Phi}{\partial \text{Range}^2}$	5.27	11.3
$\frac{\partial^2 \Phi}{\partial \text{Roll}^2}$	2.77	3.3110^{-2}
$\frac{\partial^2 \Phi}{\partial \text{Pitch}^2}$	3.30	2.2010^{-3}

	Eigenvectors		
Range	1.00	0.775	0.477
Roll	-0.723	1.00	-0.436
Pitch	-0.792	0.066	1.00

Table 11: *The diagonal of the Hessian matrix, H, and corresponding eigenvalues and eigenvectors for the three angles Roll, Yaw and Pitch.*

The second derivative, tab 11, shows that all three parameters will be well determined which is also confirmed by NAB, fig 15.

8 Discussion

When studying an optimization problem it is important to investigate the function itself as well as the results given by the optimization. A study of the derivative at the global minimum shows if one or several parameters will be hard to determine during the optimization. Such properties of the object function influence the optimization process and the choice of the optimization algorithm. For the object function used here DE has been a good choice, easy to work with and usually rapidly convergent.

Range and Depth

Both Range and Depth are well determined by a two dimensional DE search for these parameters. The second derivatives at the global minimum show that the axes of the level curves of $\Phi(\text{Range}, \text{Depth})$ are nearly parallel to the Range and Depth coordinate axes, with a ratio of ca 3 between the Depth and the Range oriented diameters. Thus Range is slightly better defined than Depth.

Roll, Yaw and Pitch

Pitch has been most easily determined out of the three angles, which is due to the box shaped scatterer. A different shape of the scatterer changes which angle that influences the fitness function the most.

When Roll, Yaw and Pitch are included in the DE optimization it is harder to get well determined values and also more difficult to reach convergence. Yaw influences the object function much less than Roll and Pitch and is thus less well defined. This is due to the box shaped scatterer and the small Yaw angles used in this study. Larger Yaw angles will have a larger influence on the fitness function.

The convergence difficulties when searching for the angles seem not to affect the accuracy of the parameters. NAB shows that all three parameters will be well determined. However with more noise in the data the accuracy of the yaw angle is expected to deteriorate faster than that of Roll and Pitch.

Density and Sound speed

The low fitness values obtained from $\Phi(\text{Density}, \text{Sound speed})$ indicates that Density and Sound speed has little influence on Φ . The second derivative at the global minimum shows that $\Phi(\text{Density}, \text{Sound speed})$ has a faint slope at the minimum. Therefore the parameters could only be well determined with a tolerance of 10^{-9} , which is not very meaningful since it would be far below the noise level in actual experimental data. To calculate the PPD with NAB noise had to be added during the DE optimization. Now, due to the low fitness values and the faint slope at the minimum, the parameters could not be determined with DE since the fitness values drowned in noise.

As with the Yaw angle, a change in the search region for the Density and the Sound speed would increase the parameter's influence on the fitness function. The search domain should in this case be chosen closer to the values of the

water, i.e. the studied inversion technique is useful for determining interior density and sound speed for softer acoustically water-like objects. Also, by using a smaller distance between the source and the receivers, a larger incidence angle will be obtained which may enhance acoustic penetration into the box, and thus increase the influence of the Density and the Sound speed on the object function.

The final test (Range, Roll and Pitch)

Range, Roll and Pitch are well suited to be optimized jointly. A larger tolerance can be used during the DE optimization without any effect on the accuracy of the end result.

In general the fewer parameters included in the optimization the better results presented by DE. Attempts to determine all seven parameters by a single DE optimization failed.

9 Conclusions

As a conclusion Range, Roll and Pitch are easily determined with DE. Depth seems to be harder to determine when the number of parameters grows and should perhaps be determined with as few other parameters as possible. Also the Yaw angle can be more well determined if a smaller number of parameters are involved during the DE optimization. These results are dependent on the chosen search domain and the specified experimental geometry. A change in either one of these will give rise to different results than stated above.

The influence of Density and Sound speed on the object function is too small for inversion for these parameters to work in the chosen search region. Investigations not included in this report indicate, however, that the Density and Sound speed of acoustically softer (more water-like) objects are identifiable by the inversion technique studied here.

References

- [1] Anton H. and Rorres C. *Elementary linear algebra*. 7th edition, pp 483-484, 1994.
- [2] Geman S. and Geman D. Stochastic relaxation, gibbs distributions and the bayesian restoration of images. *EEE Trans. Patt. Analysis Mach. Int.*, 6:721-741, 1984.
- [3] Gothäll H. and Westin R. Evaluation of four global optimization techniques (ASSA, DE, NA, Tabu Search) as applied to anechoic coating design and inverse problem uncertainty estimation. *Technical report, FOI - Swedish Defence Research Agency, Systems Technology*, FOI-R-1593-SE, March 2005.
- [4] Heath M. *Scientific computing. An introduction survey*. 2nd edition, pp 263, 2002.
- [5] Karasalo I. and Skogqvist P. Inverse bistatic acoustic scattering for identification of buried objects. *Technical report, FOI - Swedish Defence Research Agency, Systems Technology*, FOI-R-1343-SE, September 2004.
- [6] Lampinen J. Solving problems subject to multiple nonlinear constraints by the differential evolution. 2001.
- [7] Price K. and Storn R. Differential evolution - a simple and efficient adaptive scheme for global optimization over continuous spaces. TR-95-012, March 1995.
- [8] Sambridge M. Geophysical inversion with a neighbourhood algorithm -II. *Geophys. J.*, 138:727-746, 1999.
- [9] Smith A.F.M and Roberts G.O. Bayesian computation via the gibbs sampler and related markov chain monte carlo methods. *J. R. statist. Soc.*, 55:3-23, 1993.
- [10] Storn R. Differential evolution design of an IIR-filter with requirements for magnitude and group delay. TR-95-026, p 7-10, June 1995.
- [11] Home page of Differential Evolution. <http://www.icsi.berkeley.edu/~storn/code.html>.
- [12] Home page of NAB. <http://www.rses.anu.edu.au/~malcolm/na/na.html>.